MATEC Web of Conferences **32**, 04004 (2015)
DOI: 10.1051/matecconf/20153204004

Self-propelled magnesium based micromotors: synthesis and magnetic steering

Dongdong Jin[1], Jiangfan Yu[1], Ka Hei Chan[1] and Li Zhang[1,2,3,a]

[1]*Department of Mechanical and Automation Engineering, The Chinese University of Hong Kong, Hong Kong SAR, China*
[2]*Chow Yuk Ho Technology Centre for Innovative Medicine, The Chinese University of Hong Kong, Hong Kong SAR, China*
[3]*Shenzhen Research Institute (SZRI), The Chinese University of Hong Kong, Shenzhen, China*

Abstract. In this work the magnesium based Janus micromotors were prepared by an asymmetric coating of Co-Au bilayer on the surface of Mg microparticles. The micromotor could efficiently self-propel in phosphate buffer saline (PBS) with a highest speed of 221 μm·s^{-1} without any extra additives through the macrogalvanic corrosion and pitting corrosion mechanism. The influence of pH value of PBS buffer on the motion of micromotor was also investigated. Moreover, we demonstrated that the motion of micromotor could be controlled by an external magnetic field rapidly and accurately, indicating the potential application in biomedicine.

1 Introduction

Synthetic micro-/nanomotors have aroused considerable research interest owing to their various potential applications ranging from biomedical applications to environmental remediation, such as targeted delivery, biological targets isolation, pollutants sensing and remediation in waste water, and so on [1, 2]. Micro-/nanomotors can be propelled using different mechanisms, such as self-electrophoresis [3-5], self-diffusiophoresis [6], self-thermophoresis [7, 8], bubble recoiling [9, 10], and external stimuli such as electric [11], magnetic [12-14] or acoustic fields [15, 16]. Among them, autonomous motors propelled by bubbles have drawn more and more attention recently due to their efficient self-generated motion even in high ionic strength medium and body fluid [17].

Bubble-propelled motors are powered by the reaction of chemical species on the surface of motors, which can generate one-sided bubbles through asymmetric structure. Previous designs of bubble-propelled motors usually relied on the catalytic decomposition of H_2O_2 on Pt surface, and showed high-efficient movement [18, 19]. However, the employment of toxic H_2O_2 fuel has severely limited their use for biomedical applications. Therefore, micro-/nanomotors which can harvest energy from their surrounding environment without adding any fuel attract extensive attention. For instance, Gao *et al.* introduced Al-Ga/Ti Janus particles, and they were the first bubble-propelled micromotors based on metal-water reaction which could eliminate the requirement of H_2O_2 [20]. Moreover, Mg based Janus micromotors, propelled by magnesium-water reaction with the existence of chloridion or bicarbonate ion, were proposed due to their low cost, excellent biocompatibility and efficient motion [21-23].

In this study, Mg based micromotors were prepared by asymmetric coating of Co and Au on the surface of Mg microparticles, and their autonomous motion in phosphate buffer saline (PBS) were presented. Besides, the influence of pH value of PBS buffer on the motion of Mg/Co-Au Janus particle was investigated. In addition, the magnetic control of the micromotor was demonstrated using a commercialized magnetic manipulation system named MiniMag.

2 Experimental section

2.1 Synthesis of Mg/Co-Au Janus particles

To prepare the micromotors, an asymmetric coating of Co and Au was applied on the surface of Mg microsphere with reference to steps described in previous reports [21, 22] (Fig. 1). Firstly, a clean glass slide was soaked in a mixed solution of 98 wt.% H_2SO_4 and 30 wt.% H_2O_2 (volume ratio = 3:1) for 2 hours, followed by cleaning with absolute ethanol and drying at 60 °C, to make the surface hydrophilic. Secondly, 200 μL 5 wt.% PVP/ethanol was uniformly spread on the glass slide. After being dried at 60 °C, the surface of glass slide was coated with a thin PVP film. Thirdly, the surface of PVP film was wetted by ethanol, then Mg spheres with an average size of 50 μm were immediately scattered on it. After being dried at 60 °C, the Mg spheres were partially embedded in the PVP film and stick to the glass slide. Next, 100 nm Co layer and 50 nm Au layer were

[a] Corresponding Author E-mail: lizhang@mae.cuhk.edu.hk

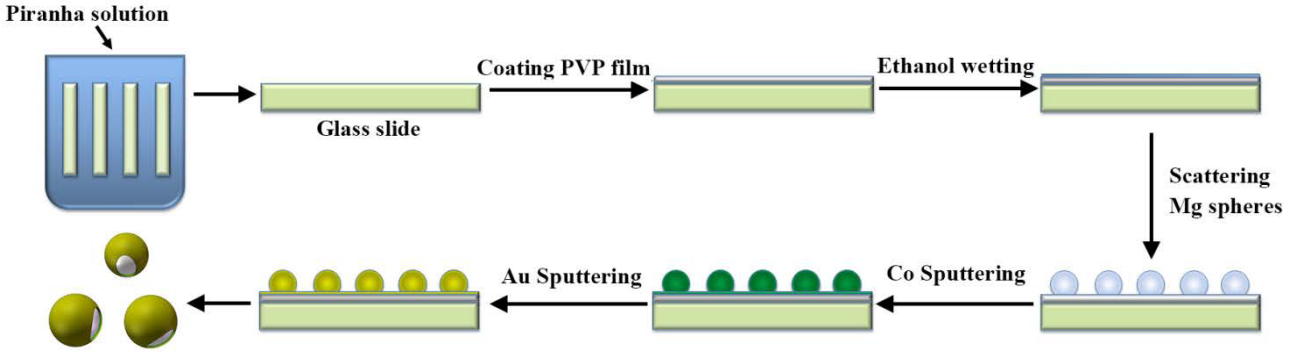

Figure 1. Fabrication of Mg/Co-Au Janus microparticles with a diameter of approximately 50 μm.

sputtered on the Mg spheres in sequence via magnetron sputtering. Finally, the partially coated Mg microparticles were released from the glass substrate by sonicating the glass slide in ethanol and stored in absolute ethanol before use.

2.2 Magnetic manipulation system

Magnetic manipulation system, named MiniMag (MagnebotiX as shown in Fig. 2(a)), is a remote electromagnetic control system with high positioning precision of the microrobots. MiniMag was used to conduct the magnetic actuation experiment with open-loop or closed-loop control. As can be seen in Fig. 2(b) and Fig. 2(c), the manipulation system has a spherical working space with a diameter of approximately 10 mm. It consists of 8 stationary electromagnetic coils with ferromagnetic cores, and is capable of 5 degree-of-freedom wireless control (3 translation and 2 orientation). The high-precision-control is accomplished by the superposition of multiple magnetic fields generated by each coil based on the order of the controller. The system is capable of generating arbitrary magnetic fields and field gradient up to 50 mT and 5 T/m at a frequency up to 2 kHz. In addition, the working principle of the magnetic manipulation system is described in Fig. 2(d).

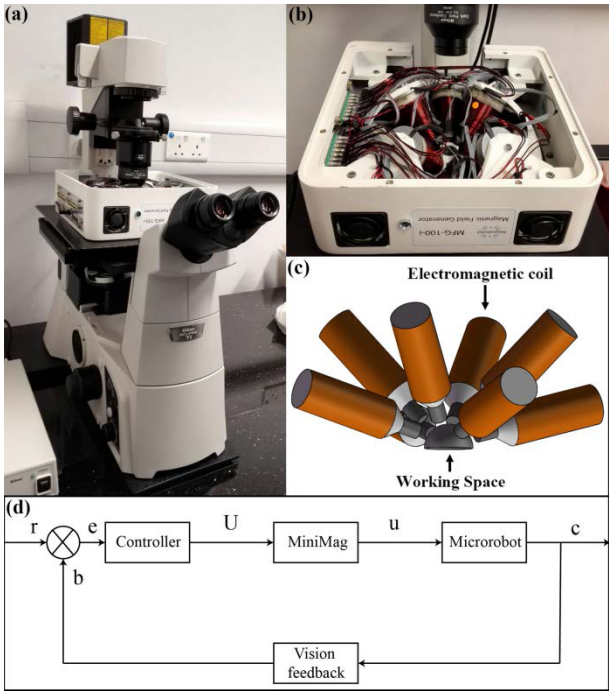

Figure 2. (a) Magnetic manipulation system – MiniMag (from MagnebotiX); (b) working space of MiniMag with 8 stationary electromagnetic coils; (c) CAD drawing of the working space; (d) Block-diagram of the working principle of MiniMag: r and b are the target position and real-time position of micromotors, respectively; e is the error of the position; U is the control signal for electromagnetic coils and u represents the generated magnetic field to control micromotors; c is the output signal.

The torque that is acting on a magnetic object exposed to an externally applied magnetic field H with a flux density $B=\mu_0 H$ (with $\mu_0=4\pi*10^{-7}$ T·m/A for the permeability of vacuum), is described by

$$T=M\times B \quad (1)$$

where M is the magnetization of the object. The torque tends to align the magnetization direction of the object with the applied field.

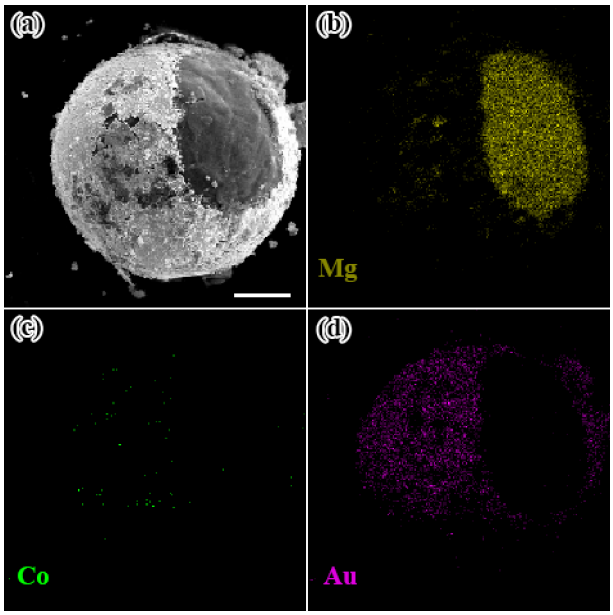

Figure 3. Scanning electron microscope (SEM) image and energy dispersive X-ray (EDX) mapping analysis of a Mg/Co-Au Janus microparticle, showing that Mg sphere was partially covered by Co and Au bilayer. The scale bar is 10 μm.

The force acting on the magnetic object can be described by

$$F=(M\cdot\nabla)B=\left[\frac{\partial B}{\partial x}\quad\frac{\partial B}{\partial y}\quad\frac{\partial B}{\partial z}\right]^{T}M \qquad (2)$$

3 Results and Discussion

The Mg/Co-Au micromotors were characterized using scanning electron microscope (SEM) and energy dispersive X-ray (EDX) spectroscopy. Fig. 3(a) showed the morphology of the as-prepared micromotor, in which more than half of the surface of Mg sphere was covered by Co-Au bilayer. The mapping EDX analysis (showed in (b), (c), (d) of Fig. 3) indicated that Co and Au could only be detected in the asymmetric coat, and Mg could be found in the opening side of the particle, further validates that Mg/Co-Au Janus particle was obtained.

To investigate the autonomous motion of Mg/Co-Au micromotors in body fluid, PBS buffer (pH=7.4) was selected as the surrounding environment of the Janus particles. The motion of micromotors was observed and recorded by an optical microscope (Nikon H600L) coupled with 4X objective and a digital camera (Grasshopper®3 GS3-U3-41C6M-C) respectively. Herein, Mg/Co-Au Janus particles was found to move efficiently in PBS buffer (shown in Fig. 4) through macrogalvanic corrosion and pitting corrosion [22]. On the one hand, the asymmetric Au layer exposed in water would facilitate the magnesium-water reaction due to its higher anodic index, and hydrogen bubbles were generated on one side. On the other hand, normally magnesium hydroxide passivation layer would be formed on the surface of Mg sphere and suppressed the consequent reaction. However, the chloridion in PBS buffer could be adsorbed in the pits on the surface of Mg sphere, where hydroxide ion would be decreased due to charge balance, thus preventing the formation of passivation layer. Therefore, hydrogen bubbles could be formed continuously and propel the micromotor for locomotion. Besides, the velocity of micromotor should be determined by the reaction rate of magnesium-water reaction, which could be regulated by several parameters, such as the concentration and pH value of PBS buffer.

Fig. 4 illustrated the irregular movement of Mg/Co-Au micromotor by a series of typical time-lapse images over a period of 17 seconds, during which, a long tail of H_2 bubbles could be found, indicating the rapid reaction between water and magnesium. In the first 5s, micromotor basically moved in a straight path. Afterwards, as a result of the fluctuation of the fluid environment (mainly generated from the magnesium-water reaction of other Janus particles) and heterogeneity of Mg spheres (asymmetric surface and mass distribution), the emission direction of H_2 bubbles changed with time, resulting in the curvilinear motion.

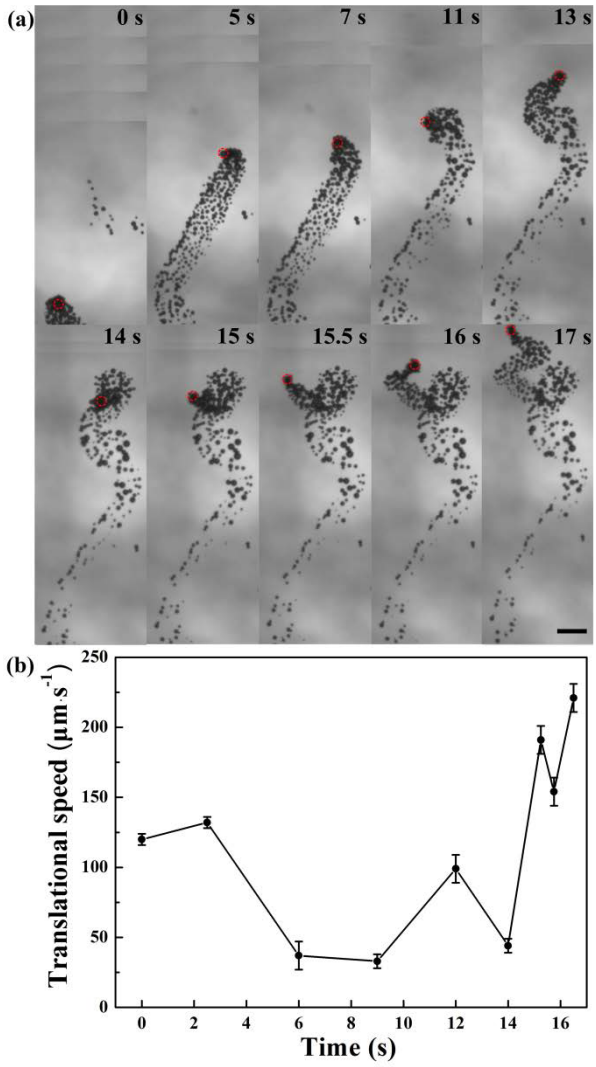

Figure 4. The autonomous movement of Mg/Co-Au Janus micromotor in PBS buffer: (a) Time lapse images illustrating the motor propulsion at 0, 5, 7, 11, 13, 14, 15, 15.5 16 and 17s intervals. The scale bar is 100 μm; (b) Translational speed of the Janus micromotor.

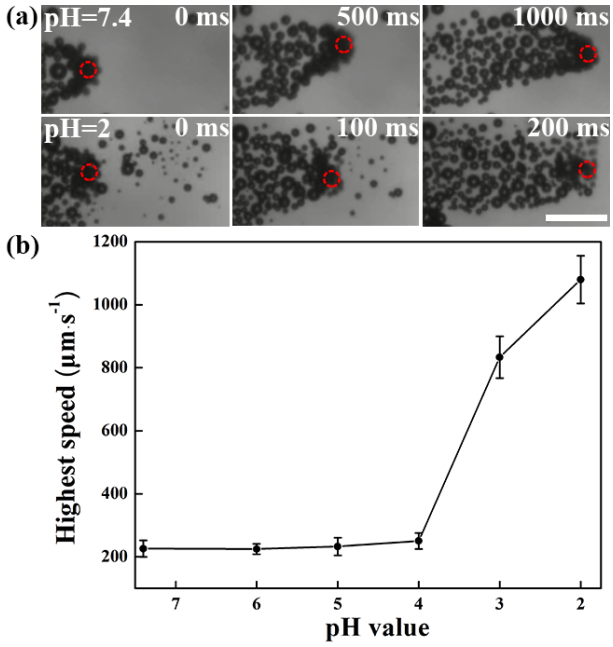

Figure 5. (a) The autonomous movement of Mg/Co-Au Janus micromotor in PBS buffer with a pH value of 7.4 and 2. The scale bar is 200 μm; (b) The highest movement speed of the Janus micromotor in PBS buffer with different pH.

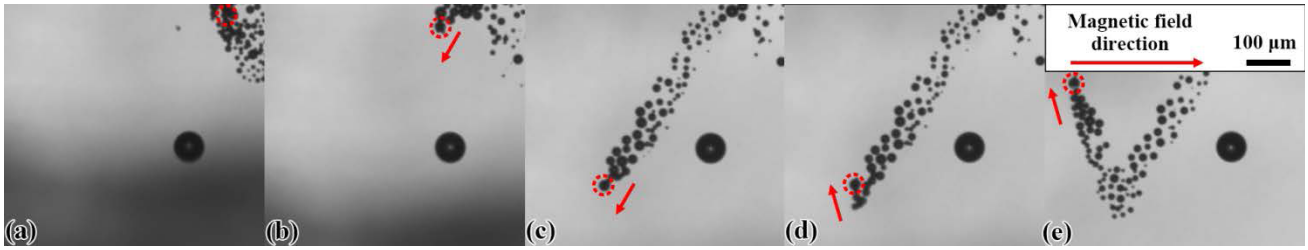

Figure 6. Magnetic control of the Mg/Co-Au Janus micromotor. The magnetic strength is 3 mT.

The movement speed of the Janus micromotor during the period was also indicated in Fig. 4. It was found that the speed of Janus particle changed with time and the highest speed reached 221 μm·s^{-1}, which corresponded to more than 4 body lengths per second. Moreover, a remarkable propulsive force of approximately 210 pN could be generated according to the following equation (3) [19],

$$F_{drag}=6\pi\mu rv \quad (3)$$

Where F_{drag} is the driving force, μ is the viscosity of fluid environment, r is the radius of micromotor and v is the movement speed of micromotor.

The influence of the pH value of PBS buffer on the movement speed of Mg/Co-Au micromotors was also investigated and the highest speed of micromotor under different solution pH was illustrated in Fig. 5. In Fig. 5(a), which exemplified the time lapse images of the autonomous movement of micromotor in PBS buffer with a pH value of 7.4 and 2, it could be observed that it took less time to travel the same distance in pH=2 solution, demonstrating that strong acidic fluid environment could facilitate the reaction between magnesium and water, and thus propel the micromotor more efficiently. Moreover, Fig. 5(b) showed that the pH value of weak acidic PBS buffer (4<pH<7.4) had a limited effect on the propulsion of micromotor, which was consistent with the previous report [22].

Fig. 6 showed the time lapse images to illustrate the magnetic steering of Mg/Co-Au Janus micromotor using MiniMag. In Fig. 6(a), there was no magnetic field and the motor was propelled along a spiral trajectory. When a magnetic field was applied, as shown in Fig. 6(b) and Fig. 6(c), micromotor turned towards the magnetic field direction and moved along a straight line parallel to the magnetic field. When the magnetic field direction was changed (as shown in (d) and (e) of Fig. 6), the micromotor would respond immediately and moved along the new direction of magnetic field. Therefore, the as-prepared magnetic Mg/Co-Au micromotors could be effectively manipulated by an external magnetic field, which was beneficial to a variety of biomedical applications.

4 Conclusions

In conclusion, the fabrication and autonomous motion of Mg/Co-Au Janus particles were presented. The micromotors could efficiently self-propel in PBS buffer with the highest speed of 221 μm·s^{-1} by the macrogalvanic corrosion and pitting corrosion mechanism. The influence of the pH value of PBS buffer on the motion of micromotor was also discussed, suggesting that only the strong acidic fluid environment could have a visible effect. Furthermore, magnetic manipulation system (MiniMag) was used to control the motion of micromotor and it was found that the magnesium Janus particles could provide a fast and accurate feedback to the exernal magnetic field, which had demonstrated potential for biomedical applications in vivo.

Acknowledgment

This work was partially supported by the early career scheme (ECS) grant with Project No. 439113 and the General Research Fund (GRF) with Project No. 417812 from the Research Grants Council (RGC) of Hong Kong SAR, the National Natural Science Funds of China for Young Scholar with the Project No. 61305124, and the grant from the Science, Technology and Innovation Committee of Shenzhen Municipality (SZSTI) for Basic Research Fund with the Project No. JCYJ20140905151415999.

References

1. J. Wang, W. Gao, ACS Nano, **6**, 5745-5751 (2012)
2. W. Gao, J. Wang, ACS Nano, **8**, 3170-3180 (2014)
3. W.F. Paxton, K.C. Kistler, C.C. Olmeda, A. Sen, S.K. St. Angelo, Y. Cao, T.E. Mallouk, P.E. Lammert, V.H. Crespi, J. Am. Chem. Soc., **126**, 13424-13431 (2004)
4. S. Fournier-Bidoz, A.C. Arsenault, I. Manners, G.A. Ozin, Chem. Commun., 441-443 (2005)
5. T. Mirkovic, N.S. Zacharia, G.D. Scholes, G.A. Ozin, Small, **6**, 159-167 (2010)
6. R.A. Pavlick, S. Sengupta, T. McFadden, H. Zhang, A. Sen, Angew. Chem. Int. Ed., **123,** 9546-9549 (2011)
7. H.R. Jiang, N. Yoshinaga, M. Sano, Phys. Rev. Lett., **105** (2010)
8. L. Baraban, R. Streubel, D. Makarov, L. Han, D. Karnaushenko, O.G. Schmidt, G. Cuniberti, ACS Nano, **7**, 1360-1367 (2013)
9. A.A. Solovev, Y. Mei, E. Bermúdez Ureña, G. Huang, O.G. Schmidt, Small, **5**, 1688-1692 (2009)

10. D.A. Wilson, R.J. Nolte, J.C. van Hest, Nat. Chem., **4**, 268-274 (2012)
11. G. Loget, A. Kuhn, Nat. Commun., **2**, 535 (2011)
12. R. Dreyfus, J. Baudry, M.L. Roper, M. Fermigier, H.A. Stone, J. Bibette, Nature, **437**, 862-865, (2005)
13. L. Zhang, J.J. Abbott, L. Dong, B.E. Kratochvil, D. Bell, B.J. Nelson, Appl. Phys. Lett., **94**, 064107 (2009)
14. W. Gao, S. Sattayasamitsathit, K.M. Manesh, D. Weihs, J. Wang, J. Am. Chem. Soc., **132**, 14403-14405 (2010)
15. W. Wang, L.A. Castro, M. Hoyos, T.E. Mallouk, ACS Nano, **6**, 6122-6132 (2012)
16. D. Kagan, M.J. Benchimol, J.C. Claussen, E. Chuluun-Erdene, S. Esener, J. Wang, Angew. Chem. Int. Ed., **124**, 7637-7640 (2012)
17. W. Gao, R. Dong, S. Thamphiwatana, J. Li, W. Gao, L. Zhang, J. Wang, ACS Nano, **9**, 117-123 (2015)
18. W. Gao, S. Sattayasamitsathit, J. Orozco, J. Wang, J. Am. Chem. Soc., **133**, 11862-11864 (2011)
19. J.G. Gibbs, Y.P. Zhao, Appl. Phys. Lett., **94**, 163104 (2009)
20. W. Gao, A. Pei, J. Wang, ACS Nano, **6**, 8432-8438 (2012)
21. F.Z. Mou, C.R. Chen, H.R. Ma, Y.X. Yin, Q.Z. Wu, J.G. Guan, Angew. Chem. Int. Ed., **125**, 7349-7353 (2013)
22. W. Gao, X.M. Feng, A. Pei, Y. Gu, J.X. Li, J. Wang, Nanoscale, **5**, 4696-4700 (2013)
23. F.Z. Mou, C.R. Chen, Q. Zhong, Y.X. Yin, H.R. Ma, J.G. Guan, ACS Appl. Mater. Interfaces, **6**, 9897-9903 (2014)